JOURNAL OF BACTERIOLOGY, Oct. 2006, p. 6953–6965 Vol. 188, No. 19
0021-9193/06/$08.00+0 doi:10.1128/JB.00681-06

Dual Role of the PhoP~P Response Regulator: *Bacillus amyloliquefaciens* FZB45 Phytase Gene Transcription Is Directed by Positive and Negative Interactions with the *phyC* Promoter†

Oliwia Makarewicz,[1] Sarah Dubrac,[2] Tarek Msadek,[2] and Rainer Borriss[1]*

Institut für Biologie, Humboldt Universität Berlin, Chausseestrasse 117, D-10115 Berlin, Germany,[1] and Unité de Biologie des Bactéries Pathogènes à Gram Positif, CNRS URA 2172, Institut Pasteur, 25 rue du Dr ROUX, 75724 Paris Cedex 15, France[2]

Received 12 May 2006/Accepted 17 July 2006

Several *Bacillus* strains secrete phytase, an enzyme catalyzing dephosphorylation of *myo*-inositol hexakisphosphate (phytate). We identified the *phyC* (phytase) gene from environmental *Bacillus amyloliquefaciens* FZB45 as a member of the phosphate starvation-inducible PhoPR regulon. In vivo and in vitro assays revealed that PhoP~P is essential for *phy*C transcription. The transcriptional start site was identified downstream of a σ^A-like promoter region located 27 bp upstream of the probable translation ATG start codon. Inspection of the *phyC* promoter sequence revealed an unusual structure. The −35 and −10 regions are separated by a window of 21 bp. A pair of tandemly repeated PhoP TT(T/A/C)ACA binding boxes was located within and upstream of the −35 consensus promoter region. A single PhoP box was found within the −10 consensus promoter region. DNase I footprinting experiments performed with isolated PhoP confirmed that PhoP~P binds at two sites overlapping with the *phy*C −35 and −10 consensus promoter region. While binding of dimeric PhoP~P at −35 is essential for activation of the *phyC* promoter, binding of PhoP~P at −10 suppresses promoter activity. A sixfold enhancement of *phyC* gene expression was registered after T:G substitution of nucleotide −13 (mutant MUT13), which eliminates PhoP binding at the single PhoP box without impairing the −10 consensus sequence. Moreover, MUT13 also expressed *phyC* during phosphate-replete growth, suggesting that the repressing effect due to binding of PhoP~P at −10 was abolished. A model is presented in which transcription initiation of *phyC* is positively and negatively affected by the actual concentration of the PhoP~P response regulator.

Phytases are enzymes that sequentially remove phosphate groups from *myo*-inositol 1,2,3,4,5,6-hexakisphosphate (phytate), the main storage form of phosphate in plants. Based on sequence homology, phytases (EC 3.1.3.8 for 3-phytase and EC 3.1.8.26 for 6-phytase) can be classified into histidine acid phosphatases, plant purple acid phosphatases, and *Bacillus* β-propeller phytases (36). Besides their ability to make phytate phosphorus available, elimination of chelate-forming phytate, which is known to bind nutritionally important minerals (Zn^{2+}, Fe^{2+}, and Ca^{2+}), is another beneficial effect of extracellular phytase activities of several soil bacteria, such as *Pseudomonas* (24), *Klebsiella* (18), and *Bacillus* spp. (25). Phytase activities of bacteria inhabiting the plant rhizosphere may contribute to their plant growth-promoting effect (23, 44). Although phytases from various microbial sources are now widely used in biotechnology, mainly in the animal feed industry to improve the bioavailability of phosphate locked in the phytins (32, 38), reports about the molecular mechanisms directing phytase expression in bacteria are scarce. One of the few studied examples is *Escherichia coli appA*, which encodes a histidine acid phosphatase with high phytase activity. The *appA* gene is a member of the *cyx appA* operon, which is regulated by anaerobiosis, phosphate starvation, and growth phase (5, 13).

Phytase genes of several *Bacillus* species have recently been cloned and characterized as single genes apparently not involved in operon structures (23–26, 48). We observed that, in contrast to the phytase genes of *Bacillus* wild-type strains, the phytase gene of *Bacillus subtilis* 168 is cryptic, most likely due to the absence of a functional promoter structure (O. Makarewicz and R. Borriss, unpublished observations).

In order to reveal the regulation network controlling phytase expression on a genetic level, we fused the environmental *Bacillus amyloliquefaciens* FZB45 phytase gene promoter and the *lac*Z reporter gene and transformed the construct as a single copy into the genetic background of *Bacillus subtilis* 168 and its derivatives. We demonstrate now that the *B. amyloliquefaciens* FZB45 phytase is a member of the phosphate starvation-induced regulon controlled by the PhoPR signal transduction system, which is directing gene expression by a combination of positive and negative interactions of the response regulator with the *phyC* promoter sequence.

MATERIALS AND METHODS

Bacterial strains, plasmids, and media. Bacterial strains and plasmids used in this study are listed in Table 1. Strains were grown in Luria-Bertani (LB) medium, low-phosphate medium (LPM), consisting of 0.1% casein peptone, 0.045% soya peptone, 0.4% glucose, 0.05% glutamate, 0.5% NaCl, 1.7 mM $MgCl_2$, 1.4 mM $MgSO_4$, 0.47 mM KCl, 0.3 mM $CaCl_2$, and 50 mM Tris-HCl at pH 7.5, and high-phosphate medium (HPM), consisting of LPM plus 10 mM phosphate. When appropriate, antibiotics were added in the following concentrations: for *E.*

* Corresponding author. Mailing address: Institut für Biologie, Humboldt Universität Berlin, Chausseestrasse 117, D-10115 Berlin, Germany. Phone: 49 30 2093 8137. Fax: 49 30 2093 8127. E-mail: rainer.borriss@rz.hu-berlin.de.

† Supplemental material for this article may be found at http://jb.asm.org/.

TABLE 1. Strains and plasmids used in this study

Strain or plasmid	Description	Reference or source
E. coli		
DH5α	*supE44* Δ*lacU169* (ϕ*80 lacZ*Δ*M15*) *hsdR17 recA1 gyrA96 thi-1 relA1*	Lab strain
C41(DE3)	F *ompT hsdS*(r m) *gal dcm* (DE3)	35
C41PhoP	F *ompT hsdS*(r m) *gal dcm* (DE3) pPHOP	This work
C41PhoR231	F *ompT hsd*(r m) *gal dcm* (DE3) pPHOR*	This work
Bacillus		
FZB45	Wild type	FZB Berlin
Bacillus subtilis		
MF1	*trpC2 pheA1* Neo^r $rpoC_{His6}$	M. Fujita
168	*trpC2*	Laboratory stock
1A254	*trpC2 pheA1 phoP*	BGSC
OM211	*trpC2 amy*::pOM2 Cm^r	This work
OM611	*trpC2 amy*::pOM6 Cm^r	This work
OM621	*trpC2 pheA1 phoP amy*::pOM6 Cm^r	This work
OM711	*trpC2 amy*::pOM7 Cm^r	This work
OM145	*trpC2 amy*::pCUT1 Cm^r	This work
OM245	*trpC2 amy*::pCUT2 Cm^r	This work
OM345	*trpC2 amy*::pCUT3 Cm^r	This work
OM445	*trpC2 amy*::pCUT4 Cm^r	This work
OM545	*trpC2 amy*::pCUT5 Cm^r	This work
MUT7	*trpC2 amy*::pMUT10 Cm^r	This work
MUT11	*trpC2 amy*::pMUT6 Cm^r	This work
MUT13	*trpC2 amy*::pMUT12 Cm^r	This work
MUT17	*trpC2 amy*::pMUT11 Cm^r	This work
MUT27	*trpC2 amy*::pMUT4 Cm^r	This work
MUT37	*trpC2 amy*::pMUT1 Cm^r	This work
MUT47	*trpC2 amy*::pMUT21 Cm^r	This work
MUT49	*trpC2 amy*::pMUT2 Cm^r	This work
Plasmids		
pDG268	Integrative vector *amy*::*lacZ* Cm^r	4
pOM2	pDG268 containing a 559-bp insert of *phyC* of *B. subtilis*	This work
pOM6	pDG268 containing a 500-bp insert of *phyC* of *B. amyloliquefaciens*	This work
pOM7	pDG268 containing a 315-bp insert of *phyC* of *B. amyloliquefaciens*	This work
pCUT1	pDG268 containing a 217-bp insert of *phyC* of *B. amyloliquefaciens*	This work
pCUT2	pDG268 containing a 252-bp insert of *phyC* of *B. amyloliquefaciens*	This work
pCUT3	pDG268 containing a 279-bp insert of *phyC* of *B. amyloliquefaciens*	This work
pCUT4	pDG268 containing a 313-bp insert of *phyC* of *B. amyloliquefaciens*	This work
pCUT5	pDG268 containing a 355-bp insert of *phyC* of *B. amyloliquefaciens*	This work
pMUT1	pOM6, transition (−37) A→G	This work
pMUT2	pOM6, transversion (−49) T→A	This work
pMUT4	pOM6, transversion (−27) T→A	This work
pMUT6	pOM6, transition (−11) A→G	This work
pMUT10	pOM6, transversion (−7) T→G	This work
pMUT11	pOM6, transition (−17) T→C	This work
pMUT12	pOM6, transition (−13) T→G	This work
pMUT21	pOM6, transversion (−47) T→G	This work
pET15b	Expression vector, Ap^r	Novagen
pET28b(+)	Expression vector, Km^r	Novagen
pPHOP	pET15b containing a 728-bp insert of *phoP* of *B. subtilis*	This work
pPHOR231	pET28b(+) containing a 1,051-bp insert of *phoR* of *B. subtilis*	This work

coli, 100 mg/liter of ampicillin (Ap) and 5 mg/liter of kanamycin (Km); for *B. subtilis*, 5 mg/liter of chloramphenicol (Cm).

DNA manipulations and general methods. Isolation of plasmid and chromosomal DNA, restriction endonuclease digestion, agarose gel electrophoresis, PCR, and transformation of *E. coli* and *B. subtilis* were performed as described previously (23).

Construction of plasmids and bacterial strains. Specific DNA fragments were amplified from the *phyC* promoter region of *B. amyloliquefaciens* FZB45 or *B. subtilis* 168 using the primer pairs listed in Table 2. The promoter-*lacZ* fusions derived from *B. amyloliquefaciens* FZB45 were cloned into the EcoRI/BamHI-digested integration vector pDG268 (4); the *B. subtilis* promoter-*lacZ* fusions were cloned into the EcoRI/HindIII-digested vector pDG268. The plasmids were linearized by XhoI digestion and transformed into competent *B. subtilis* cells (2). The transformants were screened for Cm resistance and amylase-negative phenotype. The cloned DNA regions were confirmed by sequencing.

The plasmids pMUT7, pMUT17, pMUT27, pMUT37, pMUT48, and pMUT50, which carry mutations in the putative PhoP binding sites or promoter regions, were generated using the QuikChange XL site-directed mutagenesis kit (Stratagene) according to the manufacturer's instructions. The pOM6 plasmid was used for the amplification reactions. The mutations were introduced with the primer pairs listed in Table 2 (the changed base pairs are shown in bold). The plasmids bearing the mutations were integrated into the *amyE* locus of *B. subtilis* 168 as described above.

Overexpression and purification of PhoP, PhoR, and RNA polymerase. The *phoP* gene was amplified from *B. subtilis* 168 chromosomal DNA using the primers Pho4 and Pho5. The PCR product was cloned into pGEMT (Promega)

TABLE 2. Primers used in this study

Primer	Sequence (5′→3′)	Position relative to transcription start site
Cut1	TATGTATTTTAGAATTCAAGTGAAGG	−21 to +5
Cut2	TTCACGAATTCTTAACACTGAACTTCC	−50 to −23
Cut3	TCTCCGTGAATTCTCACATGC	−81 to −58
Cut4	TATTCATTTGAATTCTTTGCTCACG	−115 to −90
Cut5	TCCGATTAATAGAATTCAAACAC	−158 to −135
F2for	AATATTTGCTCACGTCAATTTTTTTTCTCC	−104 to −75
F2rev	GTGTTTTTGAATGATTCATTTTCCTTCC	+13 to + 44
F1for	GCGAGTTAATGAAAGAAACC	−234 to −215
F3rev	GTGATAAGGATCAGACAGCTTATGC	+107 to +131
MutF7	CTTCCTGTATGTATTTTACAA**G**TAAAGTGAACG	−31 to +5
MutF17	CTTCCTGTATG**C**ATTTTACAATTAAAGTGAACG	
MutR7	GAACGTTCACTTTA**C**TTGTAAAATACATACAGG	−25 to +8
MutR17	GAACGTTCACTTTAATTGTAAAAT**G**CATACAGG	
MutF11	TTCCTGTATGTATTTT**G**CAATTAAAGTGAACG	−30 to +5
MutR11	CGTTCACTTTAATT**G**CAAAATACATACAGG	−30 to +5
MutF13	TGTATGTATT**G**TACAATTAAAGTGAACG	−26 to +5
MutR13	TTCACTTTAATTGTA**C**AATACATACAGG	−28 to +3
MutF27	CACTGAAC**A**TCCTGTATGTATTTTAC	−35 to −10
MutR27	TACATACAGGA**T**GTTCAGTGTTAAG	−40 to −16
MutF37	CGGACAATCTTCACAAAAACTT**G**ACACTGAACTTCC	−58 to −23
MutF49	CGGACAATCT**A**CACAAAAACTTAACACTGAACTTCC	
MutR37	GAAGTTCAGTGT**C**AAGTTTTTGTGAAGATTGTCCGC	−61 to −22
MutR49	GAAGTTCAGTGTTAAGTTTTTGTG**T**AGATTGTCCGC	
MutF47	ACAATCTTC**G**CAAAAACTTAACACTGAAC	−47 to −27
MutR47	AGTGTTAAGTTTTTG**C**GAAGATTGTCCG	−59 to −32
Om01	ATGAATTCCTCCAACTCTCGTTTCTCTACCATGC	−289 to −257
Om02	AATGGCAAGCTTATCTGCTGCATCATCGC	+172 to +200
Om08	CAATTAAAGTGAAGCTTCATTAAAAGGAGG	−2 to +19
Om09	ATTCTTGGGATCCAGCCAAATCG	+199 to +221
Om14	TGTTTTTGAAGGATCCATTTTCCTTCCTCC	+14 to +43
Om11	TCTTCTTCTTCTGCGATAAAGACTGCC	+684 to +709
Om16	GGATCAGACAGCTTATGCTTGCCC	+101 to +124
Pho4	GGCACCATATGAACAAAAAAATTTTAGTTG	−8 to +21
Pho5	CGCACTCGAGCTTTATTCATTCATT	+710 to 734
Om15	ATATGCGCGAATTCCTGTAGAACGAACACTAG	
RNA linker	GAUAUGCGCGAAUUCCUGUAGAACGAACACUAGAAGAAA	

to construct pGEM-*phoP*. The *phoP* gene was isolated from pGEM-*phoP* by NdeI and XhoI digestion and cloned into NdeI/XhoI-digested pET15b (Novagen), yielding pPHOP. *E. coli* C41(DE3) (34) served as a host for overexpressing the PhoP and PhoR231 proteins. Overexpression and purification of PhoP was as described previously (28). The His_6 tag was removed using the Thrombin CleanCleave kit (Sigma) according to manufacturer's instructions.

The His_6-PhoR231 protein was cloned, overexpressed, and purified as described previously (39). The expression plasmid was named pPHOR231. LB with Km was used for expression of pPHOR231.

The σ^A-containing RNA polymerase holoenzyme (RNAP) was purified as described previously (17). *Bacillus subtilis* MF1 was grown at 37°C in LB until an optical density at 600 nm (OD_{600}) of 0.8 to 1 was reached. The cells were lysed by sonification, and the holoenzyme was purified by Ni-agarose. The protein was analyzed by sodium dodecyl sulfate (SDS)-polyacrylamide gel electrophoresis and Western blotting. SDS-polyacrylamide gel electrophoresis revealed that RNA polymerase core subunits were copurified with σ^A. No other σ factors were detected (data not shown).

Enzyme assays. Overnight cultures grown without shaking in LB-Cm at 37°C were diluted in a volume of 20 ml fresh LPM or HPM to obtain an OD_{600} of 0.1 and grown at 37°C with shaking at 200 rpm. Samples (0.5 ml) were collected for the determination of optical density at 600 nm, alkaline phosphatase (APase) activity (supernatant), and β-galactosidase activity (cell pellets).

For the APase assay, 80-μl samples were solubilized with 300 μl 1 M Tris-HCl (pH 8.0) containing lysozyme (200 μg/ml), benzonase (0.1 U/ml), chloramphenicol (100 μg/ml), and 0.0005% SDS for 10 min at 30°C. Subsequently, 300 μl prewarmed *p*-nitrophenyl phosphate (1 mg/ml in 1 M Tris HCl, pH 8.0) was added to each lysed sample, and the mixture was incubated at 30°C for 5 to 15 min. The assay was stopped with 400 μl 2 M NaOH when the color had changed to yellow. Cell debris were removed by centrifugation for 5 min at 13,000 rpm, and the absorbance was measured at 410 nm. Specific APase activity was calculated as described previously (35): $U = (E_{410} \times 235 \times V_{total})/(t\ [\text{min}] \times V_{sample} \times OD_{600})$.

The β-galactosidase assay (29) was modified as follows: 100 μl of the cell suspensions were resuspended in 800 μl Z buffer (0.06 M Na_2HPO_4, 0.04 M NaH_2PO_4, 0.01 M KCl, and 0.001 M $MgSO_4$, 50 U/liter benzonase, 100 μg/ml chloramphenicol, 4 μg/μl lysozyme, and 0.0005% SDS) and incubated for 10 min at 30°C. The reaction was started with 200 μl prewarmed 2-*o*-nitrophenyl-β-D-galactopyranoside (4 mg/ml Z-buffer), and the mixtures were incubated at 30°C for 5 to 15 min. The assay was stopped by the addition of 400 μl 1 M Na_2CO_3 when the color had changed to yellow. The samples were spun for 5 min, and the

absorbance was measured at 420 nm and 550 nm. Specific β-galactosidase activity was calculated according to the method of Miller (33): $MU = 1{,}000 \times (E_{420} - 1.755) \times E_{550}/(t\ [\text{min}] \times V_{\text{sample}}\ [\text{ml}] \times \text{OD}_{600})$.

RNA analysis. Total RNA of *B. amyloliquefaciens* FZB45 was prepared using the NucleoSpin kit (Macherey-Nagel). The transcriptional start site was determined by 5′ rapid amplification of cDNA ends (RACE), following the method of Bensing et al. (7). Five micrograms of total RNA was treated with tobacco acid pyrophosphatase (Epicenter), followed by phenol-chloroform–isoamylalcohol extraction. The RNA linker (Table 2) was ligated with RNA-ligase (Epicenter). After a second extraction, the pellet was resuspended in 20 μl RNase-free water. Reverse transcription was carried out according to the Fermentas protocol using 5-μl aliquots of treated RNA, the Om09 primer (+199 to +221), and Moloney murine leukemia virus reverse transcriptase (RT) (Fermentas GmbH). The subsequent PCR was performed with 5-μl aliquots of the RT mixture, the forward primer Om15, and the nested reverse primer Om16 (+101 to +124). The PCR product was cloned into pGEMT (Promega), transformed into *E. coli* DH5α, and analyzed by sequencing.

The primer extension analysis was performed using the Moloney murine leukemia virus reverse transcriptase (Fermentas GmbH) and the [γ-^{32}P]Om16 primer according to the protocol given by the manufacturer. Total RNA of FZB45 (LPM culture) was used for the RT reaction. The sequencing reaction was performed using the Thermo-Sequenase-Cycle sequencing kit (General Electrics).

For Northern blot analysis, a *phyC*-specific DNA probe was synthesized with primers Om08 and Om11. Labeling was performed using digoxigenin and the Ready-To-Go DNA-labeling kit (Roche Diagnostics GmbH). Total RNA was separated on denaturated agarose gels and hybridized with the probe.

DNase I footprinting. DNase I footprinting experiments were essentially performed as previously described (14). A 150-bp DNA fragment corresponding to the *phyC* promoter region was obtained using primers F2for and F2rev and *Pwo* polymerase and purified with the QIAquick PCR purification kit. The PCR product was labeled on the coding strand with 5′ [γ-^{32}P]F2for and the noncoding strand by 5′ [γ-^{32}P]F2rev in separated amplification reactions and purified with the QIAquick PCR purification kit (QIAGEN). Efficiency of labeling was in the range of 300,000 to 600,000 cpm. For the DNA binding reactions, a solution of 5 mM ATP, 0.05 μg/μl bovine serum albumin, and 0.1 μg/μl poly(dI-dC) was incubated with 0, 0.05, 0.1, 0.25, 0.5, 1, or 1.5 μM PhoP in the presence or absence of 0.4 μM PhoR231 for 20 min at room temperature in binding buffer. After addition of one μl of the diluted DNA probe (adjusted to 50,000 cpm), the mixture was incubated for a further 20 min at room temperature. DNase I (0.1 U in 10 mM $MgCl_2$, 5 mM $CaCl_2$) was added to the reaction mixture, and digestion was carried out for 1 min. The reactions were stopped with DNase I stop solution (0.4 M Na acetate, 50 μg/ml calf thymus DNA [Gibco], and 2.5 mM EDTA). The samples were analyzed on a 6% polyacrylamide gel containing 7 M urea. A Maxam and Gilbert sequencing reaction mixture (cleavage reactions at purine residues A and G) (45) was loaded on the same gel.

Gel shift assay. A labeled 511-bp DNA fragment corresponding to the *phyC* promoter region was amplified using primers Om01 and 5′[γ-^{32}P]Om9 using the conditions described for footprinting. The fragment was preincubated for 10 min at room temperature with PhoP (0.2, 0.4, 0.8, or 1.6 μM), 0.1 μM PhoR231, RNAP (10, 20, or 40 nM), and 5 mM ATP in binding buffer (20 mM Tris-HCl buffer [pH 8], 100 mM KCl, 5 mM $MgCl_2$, 1 mM dithiothreitol, 10% glycerol). The binding reaction (10 μl) was initiated by addition of 15 nmol of the DNA probe (20,000 cpm) and performed for 20 min at room temperature. The reaction mixtures were separated on 6% polyacrylamide gels, prerun for 30 min at 100 V, under nondenaturing conditions in 1.5× TBE buffer (133 mM Tris base, 133 mM boric acid, 2.8 mM EDTA) at 60 V for 180 to 240 min.

In vitro transcription. The linear 511-bp templates used for in vitro transcription assays were amplified by PCR by using primers Om01 and Om09. PCR products were purified with the QIAquick PCR purification kit (QIAGEN). The in vitro transcription buffer contained 100 mM Tris-HCl, pH 8, 50 mM NaCl, 50 mM $MgCl_2$, 250 mM KCl, 5 mM $CaCl_2$, 100 μM EDTA, 5 mM dithiothreitol, and 10% glycerine. RNAP was incubated with 80 ng of template in 16 μl of transcription buffer at 37°C for 5 min. Previously phosphorylated PhoP (1.3 μM), which had been generated in binding buffer in the presence of 0.3 μM PhoR and 5 mM ATP, was added to the transcription reaction to final concentrations of 0.03, 0.06, 0.12, 0.18, 0.24, and 0.300 μM. The reaction was started by adding 4 μl of a nucleoside triphosphate mix (300 μM ATP/CTP/GTP, 0.45 μM UTP, 2 μCi [γ-^{32}P]UTP, and 40 U RNasin [Fermentas]). After incubation at 37°C for 20 min, 5 μl of stop solution (95% formamide, 30 mM EDTA, 5% glycerol, 0.05% bromophenol blue) was added. Transcripts were analyzed on 6% polyacrylamide–urea gels. A low-range RNA marker was prepared, following the protocol of Fermentas for radioactive labeling.

Sequence determination. The Thermo Sequenase Cy5 dye terminator kit (Amersham Biosciences) was used. The samples were run on ALFexpress II (Amersham Biosciences) using ReproGel High Resolution (Amersham Biosciences) and analyzed by using OMIGA 2 (Oxford Molecular) and NCBI BLAST (http://www.ncbi.nlm.nih.gov/BLAST/).

RESULTS

Transcription start and promoter sequence of the *phyC* gene of *B. amyloliquefaciens* FZB45. The coding region, including the flanking regions of the FZB45 *phyC* gene, had previously been cloned and sequenced (23). Transcription initiation was investigated by 5′ RACE as described in experimental procedures. Only RNA of the low-phosphate culture yielded a unique 124-bp PCR product consisting of the first nucleotides of the transcript at the 5′ end and ending up with the sequence complementary to the OM16 primer (Table 2) at the 3′ end. The fragment was cloned, sequenced, and confirmed to be of *phyC* origin. A transcription initiation site 27 bp upstream from the putative translation initiation codon was detected. The results obtained by 5′ RACE were corroborated by primer extension, yielding G as the first nucleotide of the *phyC* transcript (Fig. 1). The σ^A-like promoter sequence displayed an unusual structure bearing TTAACA (5/6 of −35 consensus) and TACAAT (5/6 of −10 consensus) but separated by an exceptionally large window of 21 bp which harbored in its 3′ part two direct repetitions of the sequence TGTA. At the −35 promoter sequence, two direct repeats separated by 5 bp perfectly matched the TT(C/A/T)A(C/A)A consensus PhoP binding box sequence of *B. subtilis* (16). Another putative PhoP binding box sequence was present at the −10 consensus promoter sequence, but a repeat of this sequence in an appropriate distance was missing (Fig. 1A). Almost no striking differences were detected when the sequences of the PhoP response regulators from *B. subtilis* and *B. amyloliquefaciens* were compared (85% identity). Especially, the functional domains involved in DNA binding and phosphorylation were found perfectly preserved (see Fig. SM1 in the supplemental material), suggesting that the *B. amyloliquefaciens phyC* promoter might also interact with the heterologous *B. subtilis* PhoP response regulator. The promoter structure of the FZB45 *phyC* gene is completely conserved within the upstream regions of other *B. subtilis* (25) and *B. amyloliquefaciens* (26) *phyC* genes, except that of the silent *B. subtilis* 168 *phyC* gene. Here the two tandemly arranged PhoP binding boxes were absent, while the single PhoP binding box located around the −10 promoter sequence remained conserved. Interestingly, within the *Bacillus licheniformis phyC* (48) promoter region the single PhoP box at −10 does not exist, while the two upstream-located PhoP binding boxes at −35 are well preserved (Fig. 1B).

An alternative candidate −10 promoter region was detected between −17 and −12 (TATTTT). To test the functionality of both candidate −10 regions, two different base-pair substitutions were performed and checked with the appropriate *lacZ* fusion constructs (see Fig. 7). The transversion at −7 (T→G), representing the last nucleotide of the TACAAT sequence, completely abolished the promoter activity, while the transition at −17 (T→C), representing the first nucleotide of the alternative −10 region, did not significantly affect promoter activity (see Fig. 6). These results supported the idea that the

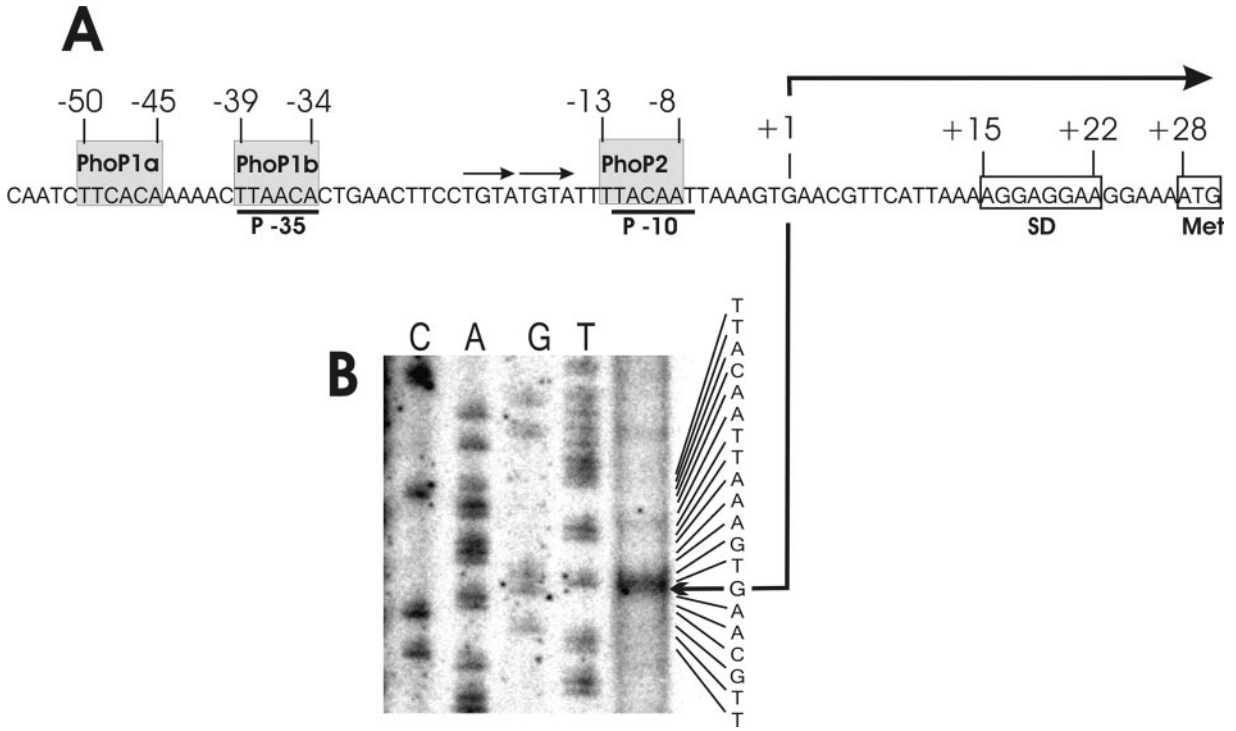

FIG. 1. Promoter structure of the FZB45 *phyC* gene. (A) Architecture of the *phyC* promoter of FZB45. Gray shading identifies the putative PhoP binding boxes. Transcriptional start site is indicated by a bent arrow. Consensus sequences (−35 and −10) are underlined. (B) Mapping of the 5′ end of the *phyC* transcript by primer extension. The CAGT sequence ladder corresponding to the nucleotide sequence of the noncoding strand is indicated at the right. The initiation of transcription (G) is marked by a bent arrow.

sequence TACAAT is the −10 region, which matches exactly with the experimentally verified transcription initiation site.

Expression of the *phyC* gene is dependent on phosphate starvation and PhoP. To study the regulation of *phyC* gene expression in *B. subtilis*, *lacZ* fusions to the *phyC* promoters of *B. subtilis* 168 and *B. amyloliquefaciens* FZB45 were ectopically integrated at the *amyE* locus. The strains were grown at three different phosphate concentrations, and the *phyC* promoter-driven β-galactosidase and the APase activities were measured throughout growth. Under low-phosphate conditions, strain OM611, harboring the FZB45 *phy*C promoter region ranging from −287 to +208, expressed β-galactosidase (Fig. 2A and B). Under medium- and high-phosphate conditions, OM611 did not express β-galactosidase. Levels of phosphate higher than 0.3 mM caused a complete arrest in formation of β-galactosidase (Fig. 2A), suggesting that expression of the *phyC* gene is strictly dependent on phosphate starvation. Similar results were obtained for activity of APase, whose induction is PhoPR dependent (22) (Fig. 2C). Northern analysis confirmed that the expression of the *phyC* gene in *Bacillus amyloliquefaciens* FZB45 is also regulated by the phosphate level. The 1.3-kb monocistronic *phyC* gene transcript was expressed only at phosphate starvation (results not shown). No reporter activity of OM211 harboring the *B. subtilis* 168 *phyC* promoter sequence was detected under any of the conditions tested.

For strain OM621, containing a *phoP* mutation rendering the strain unable to express the transcription regulator PhoP, no β-galactosidase activity was detected under low-phosphate conditions (Fig. 2B). Similarly, APase activity was totally repressed in the *phoP* mutant background, suggesting that the expression of phytase, like that of APase, is under control of the PhoP/PhoR two-component system (Fig. 2C).

We performed in vitro transcription using a purified *B. subtilis* σ^A-saturated RNA polymerase holoenzyme (see experimental procedures) and a 10 nM concentration of the *phyC* promoter fragment from pOM6 as a template to confirm the promoter-*lacZ* fusion data. The results, presented in Fig. 3A, demonstrated that transcription depends on the presence of PhoP in its phosphorylated state, as previously shown for the *phoA* gene of *B. subtilis* (42). In vitro transcription with RNAP alone (30 nM to 120 nM) yielded no visible product, but RNAP concentration-dependent transcripts with the expected size of 223 nucleotides formed in the presence of 60 nM Pho∼P. At a 60 nM concentration of RNAP and increasing concentrations of PhoP∼P (30 to 120 nM), a gradual increase of transcription efficiency was registered, but amounts of PhoP∼P exceeding 120 nM caused a sudden decrease in transcription efficiency (Fig. 3A, right). This suggested that binding of PhoP∼P at secondary sites might impede binding and/or transcription by RNAP (see later sections).

Promoter mapping. To define the regions important for activation of the FZB45 *phyC* promoter, 5′ deletions were introduced within the original 486-bp DNA fragment that contained the promoter region and the 5′ end of the coding region of the *phyC* gene (Fig. 4). These truncated *phyC* promoters were individually fused with a promoterless *lacZ* gene in pDG268. The plasmid was linearized and transformed into *B. subtilis* 168. Transformants were analyzed to ensure that the

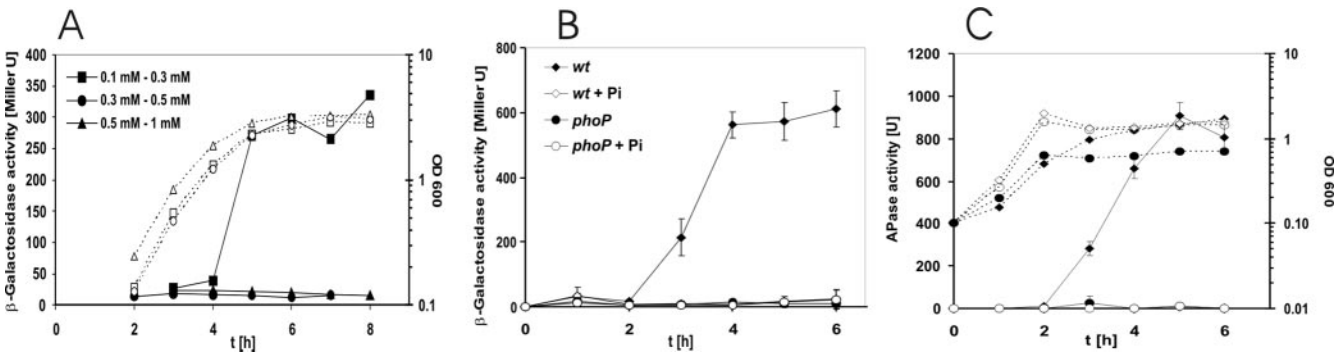

FIG. 2. Induction of APase and β-galactosidase in *phyC-lacZ* fusion strains. (A) Expression of β-galactosidase by strain OM611, which contains an FZB45 *phyC-lacZ* fusion, under three different phosphate concentrations (filled symbols). Growth of the cultures is indicated by open symbols linked by dashed lines. The symbols are given as an average range of phosphate concentrations according to measurements performed during cultivation. (B) *phyC* promoter activity in strain OM611 (wild type) (diamonds) or strain OM621 (*phoP*) (circles). Both strains were grown in LPM (solid symbols) and HPM containing 10 mM phosphate (open symbols). (C) Growth and APase activity of OM611 (diamonds) or OM622 (*phoP)* (circles) in HPM (open symbols) and LPM (solid symbols). APase activity was measured as a control for the PhoP-negative phenotype. The experiments were repeated at least three times, with similar results.

fusion was integrated as a single copy at the *amyE* locus. The activity of each promoter was determined under phosphate starvation. Deletions up to −77 did not negatively affect gene expression, while almost no activity was detected in strains where deletions were ranging up to −45 and further down. Although strain OM245 retained the complete −35 and −10 consensus boxes and two of the three PhoP recognition sites at the −35 and −10 sequence, it did not express β-galactosidase. This indicated that the presence of the PhoP box upstream of the −35 consensus sequence was necessary to confer full promoter activity. The highest level of expression was detected in strain OM345, harboring the −77 promoter deletion. This fragment contained the −35 and −10 consensus sites and all potential PhoP binding sites. Increasing the length of the 5′ upstream region gradually led to decreased reporter gene activity. Sites for a transcription repressor(s) may therefore be present within the promoter upstream region. Neither β-galactosidase nor APase activities were observed in strains growing in HPM.

A 3′ deletion that removed almost the complete coding sequence did not affect promoter activity. A −287 to +29 promoter fragment displayed the same activity as the strain harboring the entire fragment, suggesting that there are no additional regulatory sites within the coding region (Fig. 4).

PhoP∼P binds to the *phyC* promoter. Genetic and in vitro analyses described above indicated that PhoP is necessary for transcription of the *B. amyloliquefaciens* FZB45 *phyC* gene. Gel shift assays were subsequently used to analyze the binding of purified PhoP to an end-labeled 511-bp DNA fragment covering residues −290 to +221, relative to the *phyC* transcriptional start site. In these experiments, purified *B. subtilis* 168 PhoP, PhoR, and RNA polymerase were used. The functional activities of these proteins were determined with an in vitro phosphorylation assay, which confirmed that His_6-PhoR231 is autophosphorylated in the presence of [γ^{32}]ATP and that it can phosphorylate PhoP (see Fig. SM2 in the supplemental material).

Protein binding, indicated by a shift of the 511-bp promoter fragment in the presence of unphosphorylated PhoP, was not apparent even at PhoP concentrations of up to 1.6 μM, although the slight U-shaped migration in the presence of 0.8 and 1.6 μM PhoP possibly indicates some signs of binding (Fig. 5A). Interactions between unphosphorylated PhoP and DNA were demonstrated with other PhoP-dependent promoters, although these interactions were weaker than those with PhoP∼P (30). In our experiments, the complex between nonphosphorylated PhoP and the *phyC* promoter may be too labile to retard fragment migration, whereas phosphorylation of PhoP may stabilize this binding. Phosphorylated PhoP∼P bound to the promoter DNA in a concentration-dependent manner. The fragment was shifted at 0.2 μM and 0.4 μM

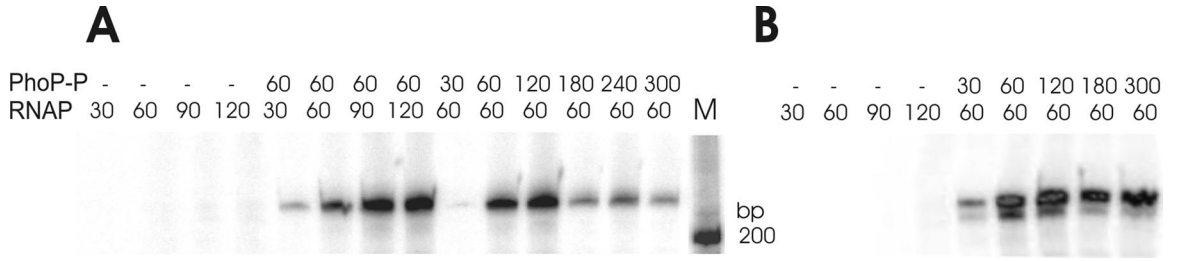

FIG. 3. In vitro transcription analysis of *phyC*. Transcription was carried out for 20 min at 37°C with purified RNAP in various amounts and a 10 nM concentration of a 511-bp *phyC* template of the wild-type (A) or MUT13 (B) promoter. PhoP (1.25 μM) was phosphorylated by 0.3 μM PhoR in binding buffer in the presence of 5 mM ATP for 20 min as described previously and was then added to the transcription reaction. The final concentrations (nM) of RNAP and PhoP-P are given at the top. M, molecular standard.

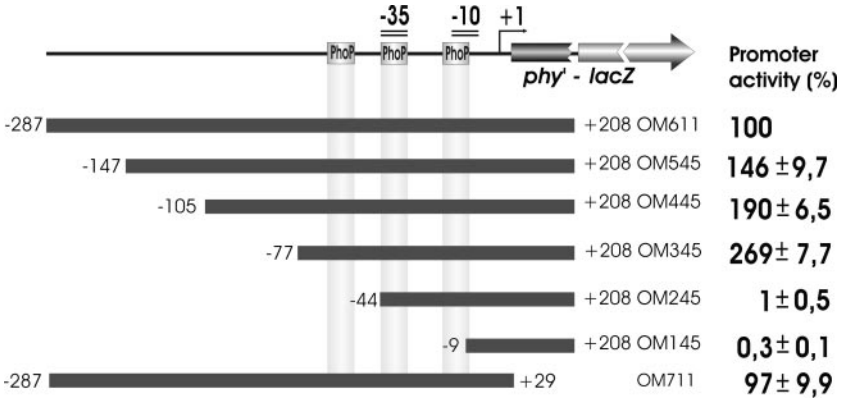

FIG. 4. Deletion analysis of the FZB45 *phyC* promoter. Top: fusion product consisting of the *phyC* promoter linked at +208 with the *lacZ* gene. Position of the PhoP boxes, of the −35 and −10 promoter sequences, and of the start point of transcription (+1) are indicated. The filled boxes represent the various lengths of the *phyC* promoter fragments used in this assay. The 5′ and 3′ ends of each fragment were labeled relative to the transcription start site, +1. The strains carrying the various truncated *phyC* promoters were grown in LPM, and the promoter activity was determined every hour. The highest activity of the reporter was obtained after 6 h and was used for calculating the relative promoter activity. The reporter activity of the full-length promoter corresponds to 100%; the activities of the other promoters are calculated as the average percentages of expression relative to that of the full-length promoter. The average mean deviation (±) was calculated from three independent experiments.

concentrations of PhoP∼P, and even more dramatic changes in mobility were observed at 0.8 μM and 1.6 μM PhoP∼P (Fig. 5A). The increased reduction of mobility may be caused by stepwise binding of PhoP∼P at PhoP boxes with different affinities and/or nonspecific binding of polymeric PhoP∼P molecules at the promoter fragment. In the absence of PhoP∼P, binding of purified RNAP (0.04 μM) at the promoter DNA was not detected (Fig. 5B). While no mobility shift occurred in the presence of unphosphorylated PhoP and RNAP (data not shown), 0.2 μM PhoP∼P shifted the promoter fragment in the presence of RNAP to a greater extent than without RNAP, suggesting that PhoP∼P and RNAP might interact cooperatively. The gel mobility shift in the presence of 0.2 μM PhoP∼P and RNAP was reproducibly more pronounced than with 0.4 or 0.8 μM PhoP∼P and RNAP (Fig. 5B). This is in agreement with the results obtained by in vitro transcription (Fig. 3A) and might suggest that higher concentrations of PhoP∼P negatively affect RNAP binding.

Interaction of PhoP and PhoP∼P with the *phyC* promoter. DNase I footprintings were performed to define the binding sites of PhoP at the *phyC* promoter. The experiments were carried out with DNA fragments amplified from the *phyC* promoter region—150 bp corresponding to the region −107 to +45—and with the purified PhoP and His_6-PhoR231 proteins. Areas of protection were only weak when unphosphorylated PhoP (≥1 μM) was added. In contrast, PhoP∼P protected two distinct promoter areas, corroborating the results obtained by mobility shifts and in vitro transcription. One region ranged from −21 to −8 at the noncoding strand and −17 to −6 at the coding strand. The second PhoP∼P-protected region was located between nucleotides −51 and −30 at the coding strand and nucleotides −59 and −34 at the noncoding strand. Two hypersensitive sites were identified at −31 and −28 on the noncoding strand and at −25 on the coding strand (Fig. 6A and B). Existence of a further binding region at around −80 cannot be ruled out, but this possibility was not substantially sup-

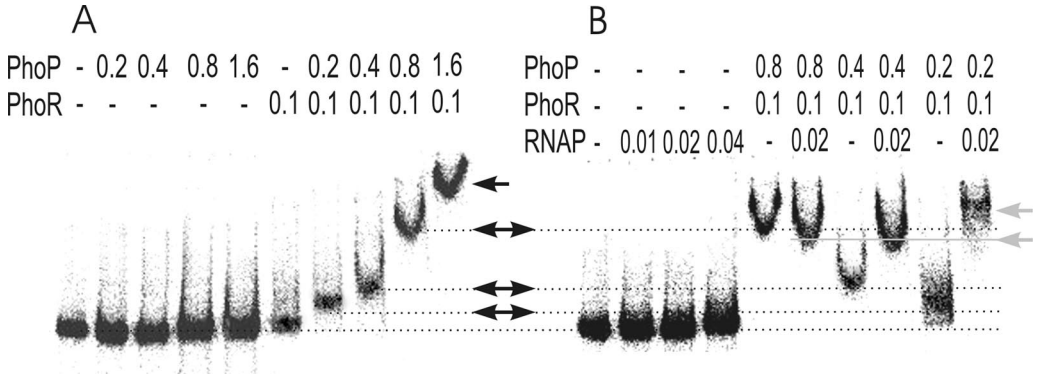

FIG. 5. Gel retardation analysis of the FZB45 *phyC* promoter by PhoP, PhoP∼P, and RNAP. The promoter DNA fragment was γ-^{32}P labeled at the 5′ end of the reverse strand. Each lane contained a 15 nM concentration of the labeled probe and 5 mM ATP. The proteins were purified as described in the text. Phosphorylation of PhoP was performed in the presence of PhoR231 and ATP. After the binding reaction with the DNA fragment, the samples were loaded on a native polyacrylamide gel in order to separate the free DNA and the DNA-protein complex. The concentrations (μM) of the proteins added to the lanes are indicated on top. The arrows indicate the different complexes.

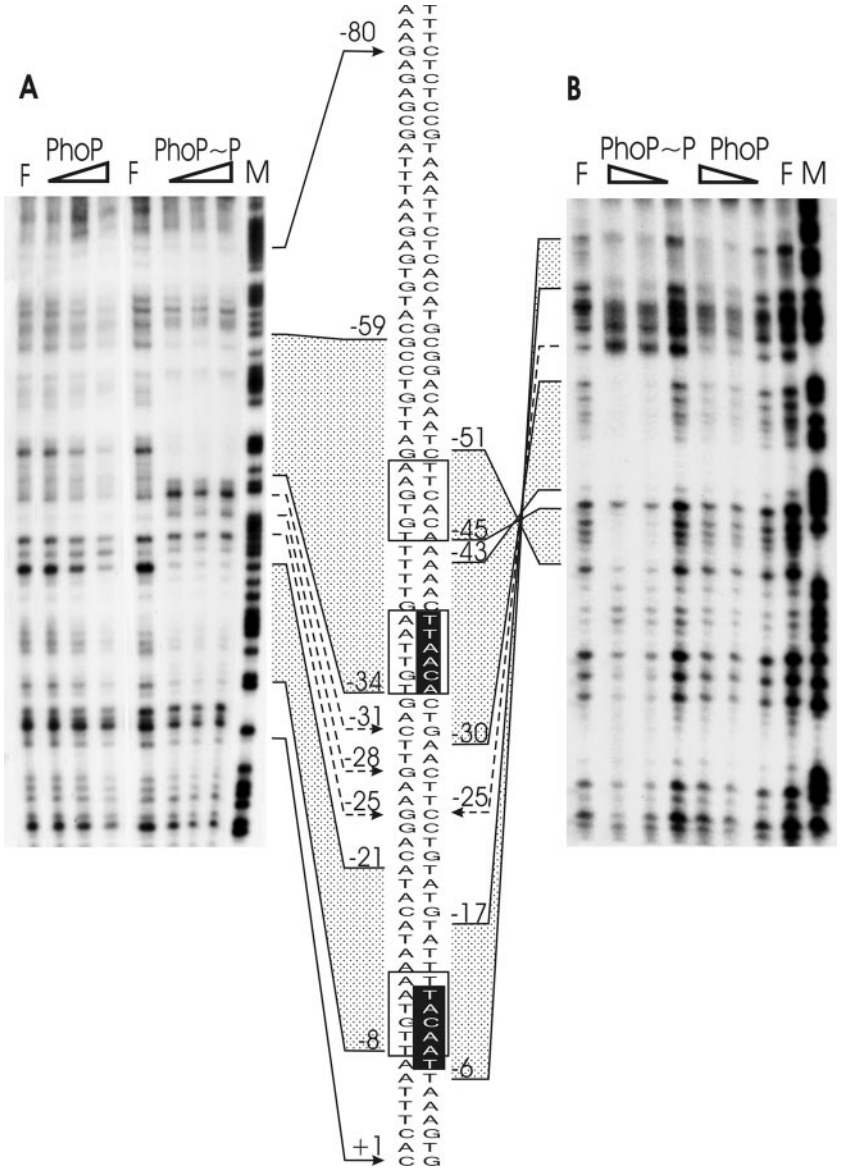

FIG. 6. DNase I footprinting analysis of the FZB45 *phyC* promoter bound by the PhoP or PhoP~P protein. A promoter fragment amplified by the F2for and F2rev primers was used to prepare the probe. Various amounts of PhoP incubated with or without PhoR231 (0.4 μM) in the presence of 5 mM ATP were mixed with the 150-bp *phyC* promoter probe, and DNase I footprinting experiments were performed with both the end-labeled noncoding (A) and coding (B) strands. F, control without protein; M, A+G-sequencing reaction. The concentrations of PhoP used in each reaction were 0.5 μM, 1.0 μM, and 1.5 μM. The gray areas represent the PhoP- and PhoP~P-protected regions at the coding (right) and the noncoding (left) strands, and the hypersensitive sites are marked with dashed arrows. The transcription start +1 site is indicated by an arrow. The corresponding sequence section is shown in the center, and the positions of interest are numbered. The PhoP recognition sites are framed, and the −10 and −35 regions are shown in white letters on a black background.

ported by the DNase I footprinting experiment shown in Fig. 6, since the control lane, F, was also weaker in the same area. Sequence analysis did not reveal any PhoP binding boxes in the sequence upstream of 51. In addition, the results of promoter mapping provided no evidence for the existence of additional PhoP binding sites within regions further upstream (Fig. 4). Therefore, we concluded that the main binding region of PhoP was located around the two PhoP boxes tandemly arranged at −50 to −45 and −39 to −34. Another binding area of PhoP~P was experimentally verified at −8 to −21, although only one PhoP binding box nearly matching the −10 consensus was detected in that area.

These results suggested that a pair of dimeric PhoP molecules might cover both promoter consensus sequences. Binding of PhoP at a single PhoP box covering the −10 consensus seems to be a unique feature of the *phyC* promoter structure and has to our knowledge not previously been reported for any other member of the PhoP/R regulon. The presence of PhoP~P-hypersensitive sites may indicate PhoP~P-dependent DNA bending.

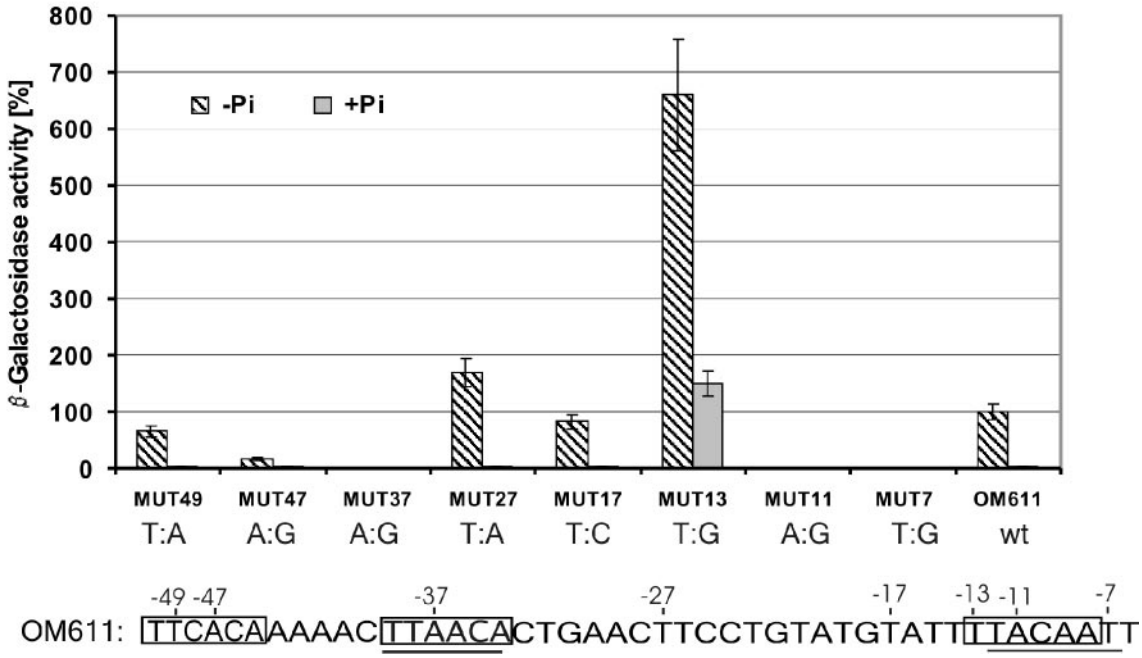

FIG. 7. Base substitution analysis within the promoter region upstream of *phyC*. The following substitutions were made: −49 (T→A), −47 (A→G), −37 (A→G), −27 (T→A), −17 (T→C), −13 (T→G), −11 (A→G), and −7 (T→G). The β-galactosidase activities of the clones were measured after 6 h of growth under high- and low-phosphate conditions. The reporter activity of the wild-type (wt) promoter corresponds to 100%; the activities of the other promoters were calculated as average percentages of expression relative to that of the wt promoter. The average mean deviation (±) was calculated from three independent experiments. Bottom: sequence of P_{phyC}. Substitutions are numbered, and the −35 and −10 regions are indicated. The putative PhoP-binding sites are contrasted by a gray background.

PhoP binding around −35 is crucial for *phyC* transcription activation. To analyze the functional importance of the two PhoP binding boxes tandemly arranged at around −47 and −35, three single-base-pair substitutions were introduced by site-directed mutagenesis (Fig. 7). As expected, nucleotide changes introduced into the −35 (MUT37) and −10 (MUT7) σ^A promoter consensus regions abolished the normal *phyC* gene expression under phosphate deprivation. Replacement of the −37 A by a G converted the conserved PhoP-binding region into a perfect promoter consensus TTGACA motif. However, no β-galactosidase activity was observed under high- or low-phosphate conditions. When nucleotide substitutions were introduced into the first PhoP binding box (MUT49 and MUT47), including the change of the A at −47 to G, only moderate reduction of transcription was observed. A→G substitutions act as one of the most deleterious substitutions in other PhoP-dependent promoters (16). According to these data, functional integrity of the second PhoP-binding site, which overlaps the consensus at −35, seems to be crucial for transcription activation, while the presence of the consensus −35 motif is less important. Conclusively, PhoP binding at −35 appears to be of more importance than RNAP binding for transcription activation.

This conclusion was examined by a DNase I footprinting assay performed with the DNA promoter fragment harboring the −37 mutation. Binding of PhoP∼P at around −35 was completely abolished. Binding of PhoP∼P at the upstream PhoP box at −47 was also negatively affected, which might indicate cooperativity in binding of PhoP dimers at this site (Fig. 8). It could be speculated that binding of the dimeric PhoP molecule occurs first at the second PhoP box located at −35, and accordingly, binding at around −47 is secondary and may be supported by protein-protein interactions after the molecule has bound at −35. However, this conclusion needs further verification by additional experiments with site-directed mutagenesis.

PhoP binding around the −10 region negatively affects *phyC* promoter activity. In order to test if the sequence TTCC located at around −27 can function as a complementary PhoP binding site, substitution of T to A at −27 was accomplished. The resulting mutant, MUT27, displayed a higher level of promoter activity (180%) than the wild-type OM611, excluding functional importance of the −27 region as a PhoP binding site (Fig. 7).

The DNase I footprinting experiments described in previous sections revealed that binding of PhoP also occurs at the −10 promoter region despite its singular PhoP box structure. In contrast to the −35 region, the single PhoP site spanning −13 to −8 does not completely match the −10 consensus, which is spanning the area −12 to −7. To dissect the functionality of this PhoP box without affecting the promoter consensus sequence, we substituted the −13 T with a G. The resulting clone, MUT13, produced more than sixfold the amount of β-galactosidase activity in LPM compared to that produced by the wild-type OM611. MUT13 also displayed *phyC* gene expression during phosphate-replete growth (Fig. 7), where the PhoP∼P concentration is very low (40). Without additional experimental data, we can only speculate that binding of a few

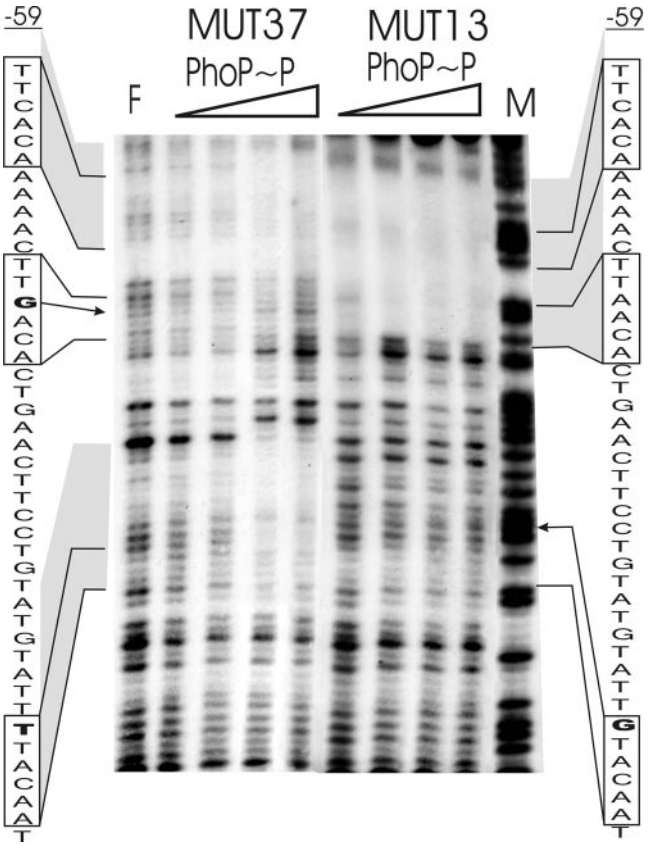

FIG. 8. DNase I footprinting analysis of mutagenized FZB45 *phyC* promoter fragments bound with the PhoP~P protein. The promoter fragment amplified by F1for and F3rev primers was used to prepare a 364-bp probe. Various amounts of PhoP incubated with PhoR231 (0.4 μM) in the presence of 5 mM ATP were mixed with the *phyC* promoter probe, and DNase I footprinting experiments were performed with the end-labeled noncoding strand. F = without protein; M = A+G-sequencing reaction lane. The concentrations of PhoP used in each reaction were 0.1 μM, 0.25 μM, 0.5 μM, and 1.0 μM. The gray areas represent PhoP~P-protected regions, the boxes indicate the PhoP recognition sites, and the letters in bold mark the substituted bases.

PhoP~P molecules is sufficient for gene expression if binding at the single PhoP box at −10 is prevented. In addition, it is possible that binding of unphosphorylated PhoP at the −35 region might support activation of the mutant *phyC* promoter under high-phosphate conditions.

DNase I footprinting analysis of this substitution revealed that PhoP~P was not bound at the mutated PhoP box around the −10 promoter region, while the PhoP boxes at around −35 and −47 were perfectly protected (Fig. 8). This suggested a dual function of the PhoP transcriptional regulator. While occupation of the PhoP boxes at the −35 region is essential for gene activation, PhoP~P binding at −10 does not support promoter activation but instead obstructs promoter RNAP interaction. Upon elimination of this additional binding site, transcription activity is strongly enhanced, but also, gene expression in the absence of PhoP~P is turned on. This idea was supported by the results of the in vitro transcription assay performed with MUT13. While transcription of wild-type *phyC* DNA was gradually suppressed in the presence of rising concentrations of PhoP~P (Fig. 3A), the same effect was not observed for MUT13. In addition, the reduction in transcription efficiency observed for the wild type at 300 nM PhoP~P was not noticed for MUT13 (Fig. 3B).

Destruction of both the −10 promoter consensus and the overlapping PhoP box prevented any transcription activity, as demonstrated with mutant MUT11, in which −11T was replaced by G. The same observation was made for the mutant MUT7, designed to selectively destroy the −10 consensus without impairing the PhoP binding box (see the previous section). An intact −10 promoter sequence is therefore crucial for *phyC* gene expression.

DISCUSSION

We show that expression of FZB45 *phyC* is controlled by the PhoPR two-component system. Generally, the PhoPR signal transduction system is induced under phosphate starvation and controls several reactions that increase the cellular supply of soil-living microorganisms with the limiting nutrient phosphate (20). including liberation of phosphate groups from *myo*-inositol hexakisphosphate by phytase. Known examples of PhoP~P-directed transcription activation in *B. subtilis* are the alkaline phosphatase genes (21) *phoA* (22) and *phoB* (12), the phosphodiesterase genes *phoD* (15) and *glpQ* (3), the gene for a high-affinity phosphate transport system, *pstS* (41), genes of the teichuronic acid synthesis operon (teichuronic acid is a cell wall polymer lacking phosphate), *tuaABCDEFGH* (29, 47), and the expression of its own operon, *phoPR* (37). PhoP~P has been shown to repress the expression of the *tagAB* and *tagDEF* genes, responsible for the production of teichoic acid (a cell wall polymer containing phosphate) (31), presumably to keep phosphate consumption on a minimal level.

Using promoter *lacZ* fusions, we demonstrated that the *phyC* gene of *B. amyloliquefaciens* FZB45 is under control of the phosphate starvation-induced PhoPR two-component system, while the *phyC* promoter of *B. subtilis* 168 is silent even under conditions of phosphate starvation. This result is supported by the observation that despite the presence of an intact coding region, the *B. subtilis* 168 *phyC* gene product is not detectable in the secretome of *B. subtilis* 168 grown under phosphate starvation conditions (3). In vitro transcription analysis established that both the $E\sigma^A$ RNAP holoenzyme and PhoP~P are necessary and sufficient to establish transcription from the FZB45 *phyC* promoter.

Data obtained with several members of the PhoPR regulon support a model in which positive regulation is exerted by binding of PhoP~P to the upstream high-affinity sites. In addition, internal sites such as those detected in the *phoA* and *pstS* genes enhance transcription initiation (42, 30). An interesting example for dual control exerted by PhoP on expression of PhoB (formerly alkaline phosphatase III) was recently reported (1). In *B. subtilis*, the *phoB* gene expression during vegetative growth under phosphate deprivation is activated by PhoP acting on an $E\sigma^A$-dependent promoter and repressed by PhoP acting on an $E\sigma^E$-dependent promoter, which is active at stage two of sporulation. As demonstrated here, the *phyC* gene from environmental *Bacillus amyloliquefaciens* is regulated by a unique control mechanism in which PhoP~P positively and negatively affects one $E\sigma^A$-responsive promoter.

Previous studies suggested that PhoP-dependent promoters possess a PhoP core binding region to which both PhoP and PhoP~P can bind (28). This ability is different from that of target sites of response regulators, such as NarL and ComA, which bind only in the phosphorylated form (43, 49). We were able to detect strong interactions between the *phyC* promoter and PhoP in its phosphorylated form, while binding between the unphosphorylated PhoP and the *phyC* promoter DNA fragment appeared to be only weak. It was shown for the *resA* promoter that unphosphorylated PhoP binds at concentrations higher than 3.4 μM (10).

PhoP binding boxes occurring in most *B. subtilis* promoters activated by PhoP consist of at least four TTAACA-like sequences repeated at specific intervals of <11 bp (28, 30). The upstream region of the *B. amyloliquefaciens* FZB45 *phy*C gene deviates from this general architecture in that there is only one appropriate binding site for the dimeric PhoP protein, which consists of two boxes centered at −47 and −35 and separated by 5 bp. This situation resembles that of the $P_{A4}E\sigma^A$ promoter of the PhoPR operon, in which only a single PhoP dimer consensus repeat exists on the noncoding strand (37). A unique feature of the *Bacillus phyC* promoter is the presence of a functional single PhoP binding box located at −13 to −8, nearly matching the −10 consensus.

There is a striking similarity in promoter anatomy of the *B. subtilis spoIIG* and *B. amyloliquefaciens phyC* genes. Despite highly conserved −35 and −10 consensus sequences, both genes are transcribed only if a dimeric phosphorylated transcription activator, Spo0A~P (11) or PhoP~P, respectively, binds at two tandemly arranged sites of either seven or six base pairs which are separated only by a few base pairs. At the *spoIIG* promoter, Spo0A~P stimulates transcription (6, 8). In vitro, RNAP binds readily, albeit weakly, to this promoter, but on linear templates it requires Spo0A~P to initiate transcription efficiently (8, 9). Similarity between both promoters is also reflected by the fact that the first of the two activator binding sites is located upstream of the −35 promoter sequence at the nontranscribed strand, while the second one is directly overlapping the −35 consensus sequence.

Optimal spacing in $E\sigma^A$-dependent promoters is 17 to 19 bp. The inability of the RNAP to transcribe *spoIIG* in the absence of Spo0A~P may be due to the large window of 22 bp separating the −35 and −10 promoter regions, effectively preventing proper binding of the enzyme to the DNA. In vitro transcription assays performed with heteroduplex templates implied that Spo0A~P stimulated transcription at least in part by stabilizing the RNA-polymerase-*spoIIG* complex until contacts between the RNA polymerase and the −10 element induced strand separation. Therefore, Seredick and Spiegelman (46) argued that the role of the transcription activator Spo0A~P is to promote alignment of σ^A with the downstream promoter elements by two possible mechanisms: (i) stimulation of the release of upstream contacts and (ii) locking of RNAP near the DNA after release from the −35 element contacts. For a recent model, Kumar et al. (27) proposed that activation of the *spoIIG* promoter is accomplished by direct interaction of the surfaces of the dimeric regulator Spo0A and $E\sigma^A$. According to their model it was unlikely that Spo0A and $E\sigma^A$ simultaneously occupy the same binding site at −35. Instead, binding of RNAP at a site with optimal spacing of 17 to 18 bp to the −10 region was favored by protein-protein contacts between dimeric Spo0A located at −35 and the RNAP bound at −10.

The sequence of another Spo0A-activated promoter, *spoIIE*, is similar to that of *spoIIG* in that it contains a −35-like box separated by 21 bp from the −10 region sequence (19). The Spo0A binding box overlaps with the −35 sequence as well (50). Due to the similarities mentioned above, we assume that a similar mechanism occurs after binding of PhoP at the −35 sequence of the *phyC* gene promoter, which possibly overcomes the steric constraints caused by improper spacing between the −35 and −10 regions.

This view is mainly supported by the results of the DNase I footprinting obtained for mutants MUT13 and MUT37 and for the PhoP~P-dependent in vitro transcription of MUT13. We suggest the following model: after first contact of the RNAP at the −35 consensus, RNAP binds directly at the −10 consensus promoter region. Most likely this event does not occur in the absence of the response regulator PhoP~P during high-phosphate conditions, due to improper spacing between the two consensus regions. During phosphate limitation, the level of PhoP~P rises, which results in occupation of the two PhoP boxes around the −35 promoter region. Protein-protein interactions between the bound PhoP~P dimer and RNAP subsequently stabilize the complex, which is linked with the promoter DNA at −10, and will finally lead to transcription activation. At high-phosphate conditions, without PhoP~P attached at −35, RNAP binding at the promoter upstream region is not supported and the *phyC* gene is not expressed. The DNase I footprinting data shown in Fig. 5 and 7 reveal higher affinity of PhoP~P to the two tandemly arranged PhoP~P boxes than to the single PhoP box at −10, suggesting first binding of the response regulator at the region adjacent to and upstream from −35. Higher levels of PhoP~P will then lead to competition between RNAP and PhoP~P at the −10 binding site and result in decreasing gene transcription. This way, *phyC* expression is relatively tightly regulated under conditions of phosphate deprivation (Fig. 9). This model is supported by our in vitro transcription experiments, in which a high concentration of PhoP reduced transcription efficiency in promoters harboring a functional PhoP binding box adjacent to −10 but was without effect in MUT13, with a mutated single PhoP box.

Future experiments may include a shortening of the window between the −35 and −10 sites, as well as identification of the amino acid residues involved in surface interactions between PhoP~P bound at the *phyC* promoter and specific $E\sigma^A$ regions of the RNAP holoenzyme. These will lead to a better understanding of the activation process of this unusual promoter structure. The promoter structure described here is well conserved in the phytase genes of *B. subtilis* VTT E-68013 (accession no. AF029053), *B. amyloliquefaciens* (accession no. U85968) and *B. licheniformis* (accession no. AF469936), suggesting that transcriptional activation of the FZB45 phytase gene is representative of *phyC* gene regulation in bacilli. In spite of these similarities, it is likely that mutations introduced within the *phyC* promoter as described here for MUT13 will be important for the design of industrial *Bacillus* strains engineered for high productivity in phytase gene expression.

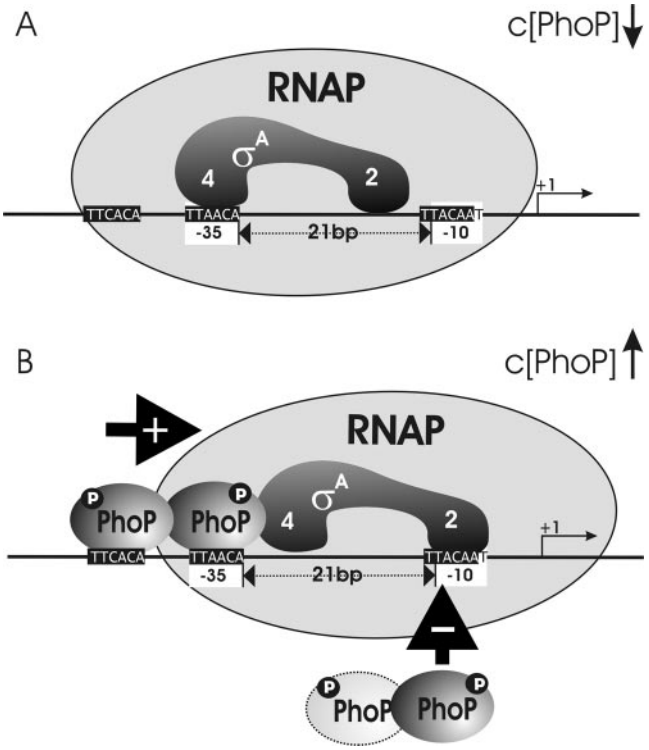

FIG. 9. Model of the interactions of PhoP and RNAP on the *phyC* promoter of *B. amyloliquefaciens* FZB45. In the absence of PhoP~P, Eσ^A RNAP binds preferentially to one of the two possible binding sites at −35 and −10 due to their improper spacing. In the presence of phosphorylated PhoP, the potential binding sites become occupied by the response regulator: the tandem repeat PhoP boxes adjacent to −35 with higher efficiency than the single one at −10. Upon binding of the dimeric response regulator PhoP~P to a region adjacent to −35, binding of RNAP at −10 is facilitated by protein-protein interactions with the upstream bound PhoP~P. Formation of open complex and transcription initiation will start. A rising concentration of PhoP~P, causing competition between PhoP~P and RNAP at −10, eventually decreases transcription efficiency. The promoter consensus sites are labeled with white, the PhoP binding sites with black boxes. The putative binding sites at subdomains Eσ^A2 and Eσ^A4 are indicated.

ACKNOWLEDGMENTS

Partial financial support given for the genomic network sponsored by BMBF, the German ministry for education and research, is gratefully acknowledged. Sarah Dubrac's work was supported by research funds from the European Commission (Grant LSHG-CT-2004-503468 BACELL Health), the Centre National de la Recherche Scientifique, and the Institut Pasteur (Grand Programme Horizontal no. 9).

We thank Masaya Fujita for providing the *Bacillus subtilis* strain MF1 used for isolation of RNAP. We also thank Christiane Müller for technical support and sequencing and Markus Wilhelms for cloning pPHOR231 and purification of the proteins. Steffen Porwollik (Sidney Kimmel Cancer Center, San Diego, Calif.) is especially thanked for valuable hints for improving the manuscript.

REFERENCES

1. **Abdel-Fattah, W. R., Y. Chen, A. Eldakak, and F. M. Hulett.** 2005. *Bacillus subtilis* phosphorylated PhoP: direct activation of the Eσ^A- and repression of the Eσ^E-responsive *phoB*-P_{S+V} promoters during Pho response. J. Bacteriol. **187:**5166–5178.
2. **Anagnostopoulos, C., and J. Spizizen.** 1961. Requirements for transformation in *Bacillus subtilis*. J. Bacteriol. **81:**741–746.
3. **Antelmann, H., C. Scharf, and M. Hecker.** 2000. Phosphate starvation-inducible proteins of *Bacillus subtilis*: proteomics and transcriptional analysis. J. Bacteriol. **182:**4478–4490.
4. **Antoniewski, C., B. Savelli, and P. Stragier.** 1990. The *spoIIJ* gene, which regulates early developmental steps in *Bacillus subtilis*, belongs to a class of environmentally responsive genes. J. Bacteriol. **172:**86–93.
5. **Atlung, T., and L. Brönsted.** 1994. Role of the transcriptional activator AppY in regulation of the *cyx appA* operon of *Escherichia coli* by anaerobiosis, phosphate starvation, and growth phase. J. Bacteriol. **176:**5414–5422.
6. **Baldus, J. M., B. D. Green, P. Youngman, and C. P. Moran, Jr.** 1994. Phosphorylation of *Bacillus subtilis* transcription factor Spo0A stimulates transcription from the *spoIIG* promoter by enhancing binding to weak 0A boxes. J. Bacteriol. **176:**296–306.
7. **Bensing, B. A., B. J. Meyer, and G. M. Dunny.** 1996. Sensitive detection of bacterial transcription initiation sites and differentiation from RNA processing sites in the pheromone-induced plasmid transfer system of *Enterococcus faecalis*. Proc. Natl. Acad. Sci. USA **93:**7794–7799.
8. **Bird, T. H., J. K. Grimsley, J. A. Hoch, and G. B. Spiegelman.** 1993. Phosphorylation of Spo0A activates its stimulation of in vitro transcription from the *B. subtilis spoIIG* operon. Mol. Microbiol. **9:**741–749.
9. **Bird, T. H., J. K. Grimsley, J. A. Hoch, and G. B. Spiegelman.** 1996. The *Bacillus subtilis* response regulator Spo0A stimulates transcription of the *spoIIG* operon through modification of RNA polymerase promoter complexes. J. Mol. Biol. **256:**436–448.
10. **Birkey, S. M., W. Liu, X. Zhang, M. F. Duggan, and F. M. Hulett.** 1998. Pho signal transduction network reveals direct transcriptional regulation of one two-component system by another two-component regulator: *Bacillus subtilis* PhoP directly regulates production of ResD. Mol. Microbiol. **30:**943–953.
11. **Burbulys, D., K. A. Trach, and J. A. Hoch.** 1991. Initiation of sporulation in *B. subtilis* is controlled by a multicomponent phosphorelay. Cell **64:**545–552.
12. **Chesnut, R. S., C. Bookstein, and F. M. Hulett.** 1991. Separate promoters direct expression of *phoAIII*, a member of the *Bacillus subtilis* alkaline phosphatase multigene family, during phosphate starvation and sporulation. Mol. Microbiol. **5:**2181–2190.
13. **Dassa, J., H. Fsihi, C. Marck, M. Dion, M. Kieffe-Bontemps, and P. L. Boquet.** 1991. A new oxygen-regulated operon in *Escherichia coli* comprises the genes for a putative third cytochrome oxidase and for pH 2.5 acid phosphatase (*appA*). Mol. Gen. Genet. **229:**341–352.
14. **Derre, I., G. Rapoport, and T. Msadek.** 1999. CtsR, a novel regulator of stress and heat shock response, controls clp and molecular chaperone gene expression in gram-positive bacteria. Mol. Microbiol. **31:**117–131.
15. **Eder, S., L. Shi, K. Jensen, K. Yamane, and F. M. Hulett.** 1996. A *Bacillus subtilis* secreted phosphodiesterase/alkaline phosphatase is the product of a Pho regulon gene, *phoD*. Microbiology **142:**2041–2047.
16. **Eder, S., W. Liu, and F. M. Hulett.** 1999. Mutational analysis of the *phoD* promoter in *Bacillus subtilis*: implications for PhoP binding and promoter activation of Pho regulon promoters. J. Bacteriol. **181:**2017–2025.
17. **Fujita, M., and Y. Sadaie.** 1998. Rapid isolation of RNA polymerase from sporulating cells of *Bacillus subtilis*. Gene. **221:**185–190.
18. **Greiner, R., E. Haller, U. Konietzky, and K.-D. Jany.** 1997. Purification and characterization of a phytase from *Klebsiella terrigena*. Arch. Biochem. Biophys. **341:**229–248.
19. **Guzman, P., J. Westpheling, and P. Youngman.** 1988. Characterization of the promoter region of the *Bacillus subtilis spoIIE* operon. J. Bacteriol. **170:**1598–1609.
20. **Hulett, F. M.** 1996. The signal-transduction network for Pho regulation in *Bacillus subtilis*. Mol. Microbiol. **19:**933–939.
21. **Hulett, F. M., E. E. Kim, C. Bookstein, N. V. Kapp, C. W. Edwards, and H. W. Wyckoff.** 1991. *Bacillus subtilis* alkaline phosphatases III and IV. Cloning, sequencing, and comparisons of deduced amino acid sequence with *Escherichia coli* alkaline phosphatase three-dimensional structure. J. Biol. Chem. **266:**1077–1084.
22. **Hulett, F. M., J. Lee, L. Shi, G. Sun, R. Chesnut, E. Sharkova, M. F. Duggan, and N. Kapp.** 1994. Sequential action of two-component genetic switches regulates the Pho regulon in *Bacillus subtilis*. J. Bacteriol. **176:**1348–1358.
23. **Idriss, E. E., O. Makarewicz, A. Farouk, K. Rosner, R. Greiner, H. Bochow, T. Richter, and R. Borriss.** 2002. Extracellular phytase activity of *Bacillus amyloliquefaciens* FZB45 contributes to its plant-growth promoting effect. Microbiology **148:**2097–2109.
24. **Irving, G. J. C., and D. J. Cosgrove.** 1971. Inositol phosphate phosphatases of microbiological origin. Some properties of a partially purified bacterial (*Pseudomonas sp.*) phytase. Aust. J. Biol. Sci. **24:**547–557.
25. **Kerovuo, J., M. Lauraeus, P. Nurminen, N. Kalkkinen, and J. Apajalahti.** 1998. Isolation, characterization, molecular gene cloning, and sequencing of a novel phytase from *Bacillus subtilis*. Appl. Environ. Microbiol. **64:**2079–2085.
26. **Kim, Y.-O., J.-K. Lee, H.-K. Kim, J.-H. Yu, and T.-K. Oh.** 1998. Cloning of the thermostable phytase (Phy) from *Bacillus* sp. DS11 and its overexpression in *Escherichia coli*. FEMS Microbiol. Lett. **162:**185–191.
27. **Kumar, A., C. Buckner Starke, M. DeZalia, and C. P. Moran, Jr.** 2004. Surfaces of Spo0A and RNA polymerase sigma factor A that interact at the *spoIIG* promoter in *Bacillus subtilis*. J. Bacteriol. **186:**200–206.
28. **Liu, W., and F. M. Hulett.** 1997. *Bacillus subtilis* PhoP binds to the *phoB* tandem promoter exclusively within the phosphate starvation-inducible promoter. J. Bacteriol. **179:**6302–6310.

29. **Liu, W., and F. M. Hulett.** 1998. Comparison of PhoP binding to the *tuaA* promoter with PhoP binding to other Pho-regulon promoters establishes a *Bacillus subtilis* Pho core binding site. Microbiology **144:**1443–1450.
30. **Liu, W., Y. Qi, and F. M. Hulett.** 1998. Sites internal to the coding regions of *phoA* and *pstS* bind PhoP and are required for full promoter activity. Mol. Microbiol. **28:**119–130.
31. **Liu, W., S. Eder, and F. M. Hulett.** 1998. Analysis of *Bacillus subtilis tagAB* and *tagDEF* expression during phosphate starvation identifies a repressor role for PhoP-P. J. Bacteriol. **180:**753–758.
32. **Lucca, P., R. Hurrell, and I. Potrykus.** 2002. Fighting iron deficiency anemia with iron-rich rice. J. Am. Coll. Nutr. **21:**184–190.
33. **Miller, J. H.** 1972. Experiments in molecular genetics. Cold Spring Harbor Laboratory Press, Cold Spring Harbor, N.Y.
34. **Miroux, B., and J. E. Walker.** 1996. Over-production of proteins in *Escherichia coli*: mutant hosts that allow synthesis of some membrane proteins and globular proteins at high levels. J. Mol. Biol. **260:**289–298.
35. **Nicholson, W. L., and P. Setlow.** 1990. Sporulation, germination and outgrowth, p. 391–450. *In* C. R. Harwood and S. M. Cutting (ed.), Molecular biological methods for Bacillus.. Wiley, Chichester, United Kingdom.
36. **Oh, B.-C., W.-C. Choi, S. Park, Y.-O. Kim, and T.-K. Oh.** 2004. Biochemical properties and substrate specificities of alkaline and histidine acid phytases. Appl. Microbiol. Biotechnol. **63:**362–372.
37. **Paul, S., S. Birkey, W. Liu, and F. M. Hulett.** 2004. Autoinduction of *Bacillus subtilis phoPR*. Operon transcription results from enhanced transcription from $E\sigma^A$- and $E\sigma^E$-responsive promoters by phosphorylated PhoP. J. Bacteriol. **186:**4262–4275.
38. **Pen, J., T. C. Verwoerd, P. A. Paridon, R. F. Beudeker, P. J. Elzen, K. Geerse, J. D. Klis, H. A. Versteegh, A. J. Ooyen, and A. Hoekema.** 1993. Phytase-containing transgenic seeds as a novel feed additive for improved phosphorus utilization. BioTechnology **11:**811–814.
39. **Pragai, Z., N. E. E. Allenby, N. O'Connor, S. Dubrac, G. Rapoport, T. Msadek, and C. R. Harwood.** 2004. Transcriptional regulation of the *phoPR* operon in *Bacillus subtilis*. J. Bacteriol. **186:**1182–1190.
40. **Puri-Taneja, A., S. Paul, Y. Chen, and F. M. Hulett.** 2006. CcpA causes repression of the *phoPR* promoter through a novel transcription start site, P_{A6}. J. Bacteriol. **188:**1266–1278.
41. **Qi, Y., Y. Kobayashi, and F. M. Hulett.** 1997. The *pst* operon of *Bacillus subtilis* has a phosphate-regulated promoter and is involved in phosphate transport but not in regulation of the Pho regulon. J. Bacteriol. **179:**2534–2539.
42. **Qi, Y., and F. M. Hulett.** 1998. PhoP~P and RNA polymerase σ^A holoenzyme are sufficient for transcription of Pho regulon promoters in *Bacillus subtilis*: PhoP~P activator sites within the coding region stimulate transcription in vitro. Mol. Microbiol. **28:**1187–1197.
43. **Roggiani, M., and D. Dubnau.** 1993. ComA, a phosphorylated response regulator protein of *Bacillus subtilis*, binds to the promoter region of *srfA*. J. Bacteriol. **175:**3182–3187.
44. **Sajidan, A., A. Farouk, R. Greiner, P. Jungblut, E.-C. Müller, and R. Borriss.** 2004. Molecular and physiological characterisation of a 3-phytase from soil bacterium *Klebsiella* sp. ASR1. Appl. Microbiol. Biotechnol. **65:**110–118.
45. **Sambrook, J., E. F. Fritsch, and T. Maniatis.** 1989. Molecular cloning: a laboratory manual, 2nd ed. Cold Spring Harbor Laboratory Press, Cold Spring Harbor, N.Y.
46. **Seredick, S. D., and G. B. Spiegelman.** 2004. The *Bacillus subtilis* response regulator Spo0A stimulates sA dependent transcription prior to the major energetic barrier. J. Biol. Chem. **279:**17397–17403.
47. **Soldo, B., V. Lazarevic, M. Pagni, and D. Karamata.** 1999. Teichuronic acid operon of *Bacillus subtilis* 168. Mol. Microbiol. **31:**795–805.
48. **Tye, A. J., F. K. Siu, T. Y. C. Leung, and B. L. Lim.** 2002. Molecular cloning and the biochemical characterization of two novel phytases from *B. subtilis* 168 and *B. licheniformis*. Appl. Microbiol. Biotechnol. **59:**190–197.
49. **Walker, M. S., and J. A. DeMoss.** 1994. NarL-phosphate must bind to multiple upstream sites to activate transcription from the *narG* promoter of *Escherichia coli*. Mol. Microbiol. **14:**633–641.
50. **York, K., T. J. Kenney, S. Satola, C. P. Moran, Jr., H. Poth, and P. Youngman.** 1992. Spo0A controls the σ^A-dependent activation of *Bacillus subtilis* sporulation-specific transcription unit *spoIIE*. J. Bacteriol. **174:**2648–2658.